ORIGINAL ARTICLE

Changing the paleo-depositional environment in the last 2300 years: a study through sedimentology and geochemistry of a sediment core, western Bay of Bengal

Janhavi Kangane[1] · Ganapati N. Nayak[1] · Anoop Kumar Tiwari[2] · S. M. Saalim[2]

Abstract

The sediment core collected at a water depth of 260.2 m off Mahanadi, western Bay of Bengal was analyzed for grain size fractions, clay minerals, and major and trace elements to understand changing depositional environments, source and processes with time, from ~ 2300 cal yr before present (BP) to the year of the collection (2014). Age was estimated using accelerator mass spectrometer (AMS) ^{14}C dates of two planktonic foraminifera samples. The core was divided into six distinct zones based on the significant changes in the sediment components and clay minerals. The presence of higher than average clay and smectite and lower silt and illite, in Zone II (2000 years BP–1070 cal yr BP) and Zone V (300–130 cal yr BP) revealed their deposition in low energy conditions, while, Zone III (1070 to 530 cal yr BP) and Zone VI (132 cal yr BP to present) exhibited higher silt and illite and lower clay and smectite than average suggesting their deposition in a high energy environment. Similar depositional environments observed between Zones II and V and also between Zones III and VI indicated the reoccurrence of similar hydrodynamic conditions with time. Zone II represents the Roman Warm Period and part of the early Medieval Warm Period, while, zone V corresponds to the retreating phase of the Little Ice Age. High Al in zone III and fluctuating trend in zone VI indicates higher Al release along with silt and illite from physical weathering in a cold and arid climate, while, smectite showed a positive correlation with Ti indicating the source of Ti and smectite as basic igneous rocks released during the enhanced southwest monsoon and warm climate. Mn and Zn distribution revealed fluctuations in the Oxygen Minimum Zone (OMZ) intensity to changing hydrodynamic conditions and depositional environments. The present study revealed changing depositional environments in the western Bay of Bengal with time with respect to changing material influx, reflecting fluctuating monsoons and climate.

Keywords Depositional environment · Hydrodynamic conditions · Paleoclimate · Sediment core · Bay of bengal

Introduction

The study of paleo-depositional environments is useful in understanding hydrodynamic conditions that prevailed during the time of sediment deposition and in turn, it can provide information on climatic conditions of the past. Hydrodynamic conditions vary spatially and temporally as a result of a change in intensity of rainfall, frequency, and intensity of storms, and possibly climate change. The distribution of sediment particles and depositional conditions in an aquatic environment is controlled by the hydrodynamic conditions (Dessai and Nayak 2007; Yang and Shi 2009). The sediment characteristics viz., grain size, clay mineralogy, and metal concentrations are often used to understand the provenance, transportation, and depositional processes of sediments in an aquatic environment (Avinash et al. 2016; Nasnodkar and Nayak 2019). Therefore, the study of sediment characteristics will reveal the hydrodynamic conditions that lead to the deposition of sediments.

The present study focuses on the Bay of Bengal, which is a shallow northern extension of the Indian Ocean. Most of the major rivers of India namely Ganga, Brahmaputra, Mahanadi, Godavari, and Krishna drain into this bay.

✉ Ganapati N. Nayak
  gnnayak@unigoa.ac.in; gnnayak57@gmail.com;
  nayak1006@rediffmail.com

[1] Marine Science, School of Earth, Ocean and Atmospheric Sciences, Goa University, Goa 403206, India

[2] National Centre for Polar and Ocean Research, Vasco da Gama, Goa, India

Among all the peninsula rivers which drain into the Bay of Bengal, Mahanadi is the second most important river for sediment and water discharge (Chakrapani and Subramanian 1990). The sediment particles from the catchment area are transported onto the adjacent continental shelf through this river and the terrigenous sediments get deposited on the continental shelf and slope. The deposited material constitutes sediment particles and nutrients with major and trace metals. Alagarsamy and Zhang (2005) have used grain size, organic carbon, and metal concentration of a sediment core to understanding provenance, weathering mechanism, and metal abundance in sediments. Moreover, the source, transportation mechanism, and depositional conditions of sediments were determined through the application of clay minerals by Naidu et al. (1995). The metal concentrations in the marine sediment core were used earlier by Calvert and Pedersen (1993) to understand the processes which control metal source and remobilization.

The monsoon is one of the important weather phenomena which have direct impacts on socio-economic conditions. Therefore, an attempt to study paleoclimate using different proxies to understand the variability of the monsoon on a longer time scale (Gasse et al. 1996; Thompson et al. 1997; Fleitmann et al. 2003) is important. The Indian sub-continent experiences both southwest (SW) and northeast (NE) monsoons of varying intensity and the sediment released to the Bay of Bengal during these two monsoons will have different characteristics. Recently several attempts have been made in the Bay of Bengal to understand the monsoon variability (Suokhrie et al. 2018; Weber et al. 2018), metal input (Banerjee et al. 2019), varying productivity, provenance (Bejugam and Nayak 2017; Prajith et al. 2018), and sediment transportation mechanism and weathering intensity (Symphonia and Nathan 2018).

Further, Datta et al. (2000) studied the grain size characteristics in the Bay of Bengal and stated that the Peninsula Rivers drained coarse sediment into the Bay of Bengal as compared to the Himalayan Rivers. Tripathy et al. (2014) suggested a decrease in sediment yield from Himalayan Rivers during the last glacial maxima (LGM) and they have related lowering of sediment supply from the Himalaya during the LGM to reduction in exposure area for weathering due to higher extent of glacier cover and weakening of south-west monsoon as a function of climate change. Shifts in sediment sources due to the changes in climate since early Holocene was reported by Prakash Babu et al. (2010) based on the granulometric, geochemical, and mineral magnetism data of the sediment cores from the eastern Bay of Bengal. Also, the distribution and preservation of metals in the core sediments of the Bay of Bengal were attributed to the changing climate conditions (Mazumdar et al. 2015). Earlier, Sarin et al. (1979) have reported the influence of high sedimentation rates, with respect to higher weathered material input

from the Indian sub-continent, in metal concentrations in the continental shelf sediments. Further, they have demonstrated a strong correlation of Al with elements Fe, Mg, and Cr, revealing their supply from continental aluminosilicates to the Bay of Bengal. Demina et al. (2019) reported that the concentration of terrigenous elements viz. Al, Ti, Si, Cr, Zn were higher during glacial periods when compared to interglacials. Further, they added that the concentration of some elements and ratios of some elements exhibit rhythmic variation representing glacial and interglacial periods highlighting the role of climate change with time. These studies indicate a continuous change in the amount and source of the supplied sediment to the Bay of Bengal under the influence of climatic controls. Therefore, studying the source and depositional process in a sediment core will help to understand the climatic history.

In the present study, an attempt has been made to understand the changing depositional environments with time (last 2300 years) using sedimentological, mineralogical, and geochemical parameters with respect to the changing influx of material from source areas in a sediment core collected off the Mahanadi river mouth. The main aim of this study was to find a correlation between changes in the sediment components, clay minerals, and geochemical elements of sediments and the paleoclimate fluctuations/monsoons.

Study area

The study area lies along the western Bay of Bengal, off the Mahanadi river mouth region (Fig. 1). The Mahanadi River is bounded by Central Indian hills in the north, the Eastern Ghats in the south and east, and by the Maikala range in the west. The drainage basin of the Mahanadi River is spread out over an area of approximately 1.42×10^5 Km^2 (Mazumdar et al. 2015) with charnockites, granites, gneisses, volcanic and sedimentary rocks. The coastal region of the Mahanadi experiences a subtropical climate with a temperature of
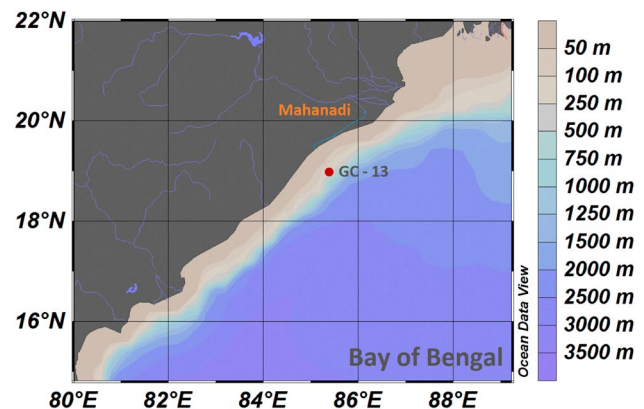

Fig. 1 Map showing the sampling location

about 21 °C and 29 °C in winter and summer respectively (Hart 1999). The catchment area receives an annual rainfall of 142 cm, 90% of which is contributed (Sundaray et al. 2006, 2011; Chakrapani and Subramani 1990) by the southwest monsoon which starts by mid-June and continues until September. The immense annual freshwater runoff of $50*90^9$ m^3 (Dixit et al. 2013; Panda et al. 2006; Konhauser et al. 1997) received by the Mahanadi influences the stratification of the water column (Levitus and Boyer 1994; Benshila et al. 2014; Suokhrie et al. 2018) in the western Bay of Bengal. Thus, high rainfall and constant inflow of water prohibit the mixing of waters, making an ideal condition for atmospheric depression. Therefore, the formation of depressions is common in the Bay of Bengal.

Materials and methods

Sampling and Collection

The sediment core (GC 13) collected at Latitude18º 99′ N and Longitude 85º 38′E in the western Bay of Bengal at 260.2 m water depth using a gravity corer onboard RV Sagar Kanya (Cruise no. 308) in January 2014 by the National Institute of Oceanography, Goa was subsampled onboard at 1 cm intervals and immediately stored in a frozen condition using plastic bags. The samples were transported to the laboratory and stored in a cold storage unit before analysis. Later, samples were oven-dried at 60 ºC. For the present study, alternate samples of the top 100 cm of the sediment core were analyzed.

Laboratory analysis

Textural analysis

The sediment sample was washed with distilled water to remove salinity and later treated with 10% sodium hexametaphosphate to dissociate clay particles and hydrogen peroxide to oxidize the organic matter. The pipette method (Folk 1968) was used to determine the percentage of sand, silt, clay which is based on Stoke's law of settling velocity principle.

Clay mineral analysis

Clay mineral analysis was carried out following the procedure given by Rao and Rao (1995). Clay slides were prepared by spreading clay (1 ml) over pre-numbered slides. Further, these slides were glycolated using ethyl glycol vapors and later scanned from 3º to 30º 2Ө at 1.2º 2Ө/min on Rigaku Altima IV X-ray diffractometer using nickel- filtered CuKα radiation. Further, clay minerals were identified and

quantified using the procedure detailed by Biscaye (1965). The smectite crystallinity was measured from the ratio between the valley height (V) and peak height (P). Illite crystallinity or Kubler index (Frey 1987) was calculated by measuring the full width at the half peak height of illite. Illite chemistry was calculated from the ratio of the area under 5 Aº and 10 Aº peak.

Bulk metal analysis

For bulk/total metal analysis grounded sediment samples were digested following the total decomposition procedure given by Jarvis and Jarvis (1985). Samples were digested using HF, HNO_3, and $HClO_4$ acid mixture with a ratio of 7:3:1 in Teflon vessel and analyzed on Atomic Absorption Spectrophotometer (AAS) (Thermo Scientific- SOLAAR M6 AAS model). Together with the samples, certified reference standard JLK-1 from the Geological Survey of Japan was digested and run, to test the analytical accuracy of the method. The average recoveries were 96.2% for Al and Fe, 94.2% for Ti, 95.3% for Mn, and 97.1% for Zn and Pb. Internal chemical standards obtained from eMerck were used to calibrate the instrument and recalibration checks were performed at regular intervals.

^{14}C accelerator mass spectrometer (AMS) dating method

The planktic foraminifera was picked from two sediment samples (> 63 μm size fraction) for measurement of AMS^{14}Cage. The dating procedure was executed at the Centre for Applied Isotopic Studies, the University of Georgia, USA, and calibration of ^{14}C ages was carried out using the Marine13 dataset (Reimer et al. 2013) drawn from Calib 7.1 (Stuiver et al. 2017) online calibration program. The top of the sediment core was assigned the year of core collection (2014) assuming that it was an undisturbed core. Further, assuming a constant rate of sedimentation between the obtained dates, the age of the remaining samples was calculated.

Results

Age of the sediment core

The ^{14}C accelerator mass spectrometer dates and rate of sedimentation are presented in Table 1 and the age-depth relationship is shown in Fig. 2. The rate of sedimentation was calculated from the dates obtained. The rate of sedimentation was 0.033 cm/ year between 100 and 50 cm whereas it was 0.064 cm/year between 50 cm and the surface, suggesting a lower sedimentation rate from 2300 cal yr before

Table 1 ^{14}C AMS dates of core GC 13

Lab code	Sample interval (cm)	14C age (year BP)	Calibrated Age (median probability) (year BP)
X30565	49–50	1156	767
X30566	99–100	2556	2297
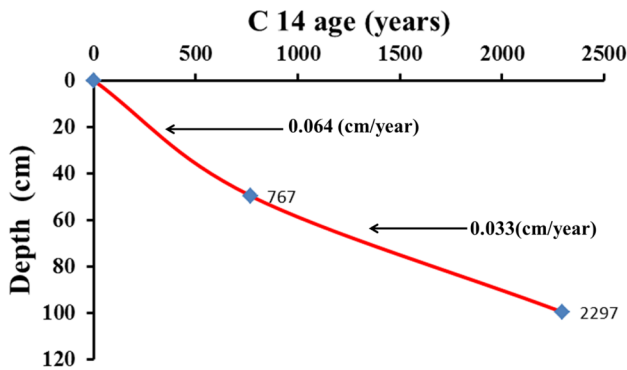
Fig. 2 Age—Depth curve

Table 2 Range and average values of sediment components

Depth (cm)		Sand (%)	Silt (%)	Clay (%)
	Core Min	0.024	24.240	9.132
	Core Max	2.548	89.040	75.206
	Core Avg	0.509	66.105	33.386
0–9	Zone VI Avg	0.308	67.952	31.740
10–21	Zone V Avg	0.339	64.380	35.281
22–35	Zone IV Avg	0.169	80.880	18.951
36–61	Zone III Avg	0.414	69.579	30.007
62–91	Zone II Avg	0.611	55.792	43.598
92–100	Zone I Avg	1.319	68.240	30.441

present (BP) to 770 cal yr BP and an accelerated rate of sedimentation in recent time from 770 cal yr BP to the present.

Grain size

The range and average amounts of sediment fractions for the core GC-13 are presented in Table 2. Sand, silt, and clay varied in the range from 0.024 to 2.548%, 24.240 to 89.040%, and 9.132 to 75.206% with the average value of 0.509%, 66.105%, and 33.386% respectively. In general, over 95% of the sediment is comprised of finer fractions i.e. silt and clay. Based on the distribution of sediment components the core was divided into six distinct zones from bottom to surface and are numbered as zone I, zone II, zone III, zone IV, zone
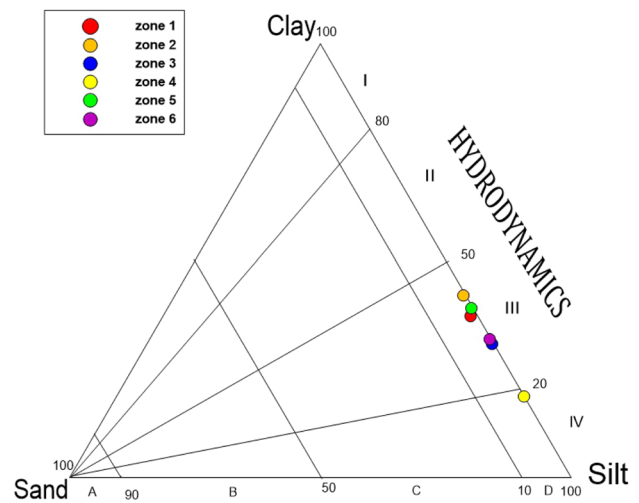
Fig. 3 Ternary diagram for classification of hydrodynamic conditions using sediment components (Pejrup 1988)

V and zone VI (Table 2). Further, to understand the hydrodynamic energy conditions of deposited sediments, average sand, silt, and clay of each zone was plotted on a ternary diagram (Fig. 3) proposed by Pejrup (1988). This diagram is used to interpret hydrodynamic conditions that prevailed during sedimentation. The subdivisions in diagram I to IV and A to D, are based on the combined effect of current velocity, wave turbulence, and water depth (Pejrup 1988). The diagram delineates four hydrodynamic sections namely I, II, III, IV which corresponds to the increasing energy, and divisions A, B, C, and D represent depositional environments with respect to textural classification. In the core GC 13, most of the data points fell in hydrodynamic class III D which represents relatively less violent hydrodynamic conditions, except zone IV which fell in class IV D representing violent hydrodynamic conditions. The data plotted (Fig. 3) indicated a close cluster or overlap of zone II and zone V, and also of zone III and VI indicating sediment deposition in similar hydrodynamic conditions and depositional environments of these zones.

The sediment component data plotted with depth is represented in Fig. 4. In the lower part of the core, zone I, showed a drastic decrease in sand and silt, and clay compensated them with depth (Fig. 4). In zone II, a uniform decreasing trend of sand, fluctuating with lower than average silt and fluctuating with higher than the average clay was observed. Silt concentration was higher and clay concentration was lower than the average in zone III. Sand maintained lower than the average concentrations in this zone. In zone IV, the silt concentration was higher and clay showed lower values than that of zone III. In zone V, a sudden change of sediment components was noted with silt fluctuating with overall lower than average values while clay fluctuated with
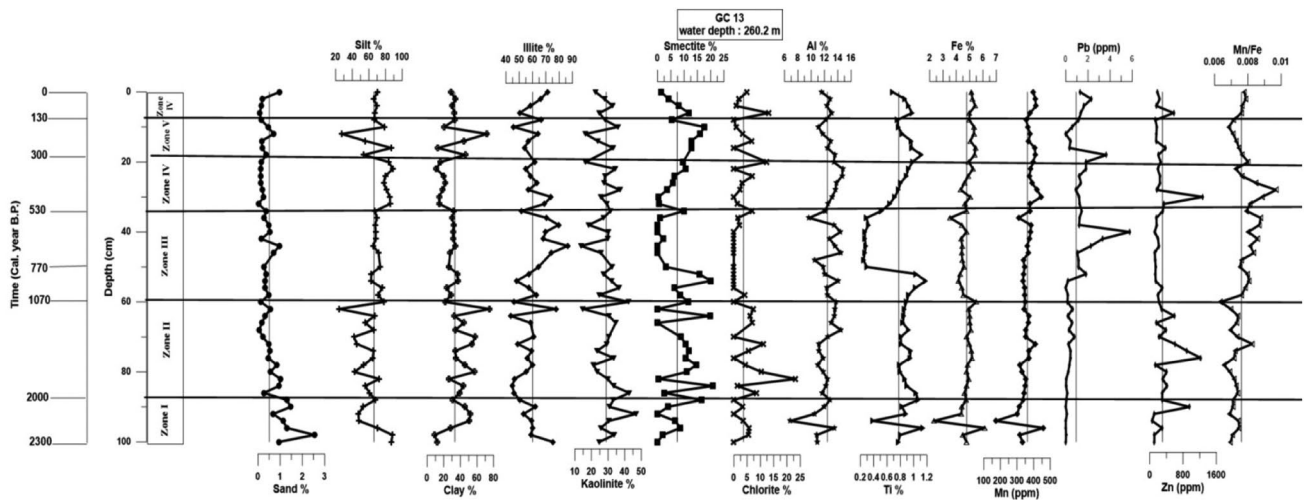
Fig. 4 Down core variation of sediment components, clay minerals and bulk metal content with zones

Table 3 Age estimated – Chronology of core GC 13

Sample Interval (cm)	Age (Cal yr B.P.)	Zone	Depth (cm)	Age (Cal yr. B.P.)
0–1	0	VI	0–9	0–130
9–10	130	V	10–21	130–300
21–22	300	IV	22–35	300–530
35–36	530	III	36–61	530–1070
49–50	770			
61–62	1070	II	62–91	1070–2000
91–92	2000	I	92–100	2000–2300
99–100	2300			

Fig. 5 Chronological model

higher than average values. Sand remained lower than average throughout this zone. In the upper zone VI, silt and clay were on their respective average line.

Chronology model

The chronology model was developed employing estimated age and is presented in Table 3 and Fig. 5. Zone I of the core corresponds to 2300 to 2000 cal yr BP, zone II from 2000 to 1070 cal yr BP and zone III represents 1070 to 530 cal yr BP. Further, Zone IV corresponds to 530 to 300 cal yr BP, Zone V from 300 to 130 cal yr BP while upper zone VI represents 130 cal yr BP to present.

Clay minerals

The range and average content of clay minerals for core GC 13 are presented in Table 4. Smectite, illite, kaolinite and chlorite varied in the range from 0 to 20.745%, 43.537 to
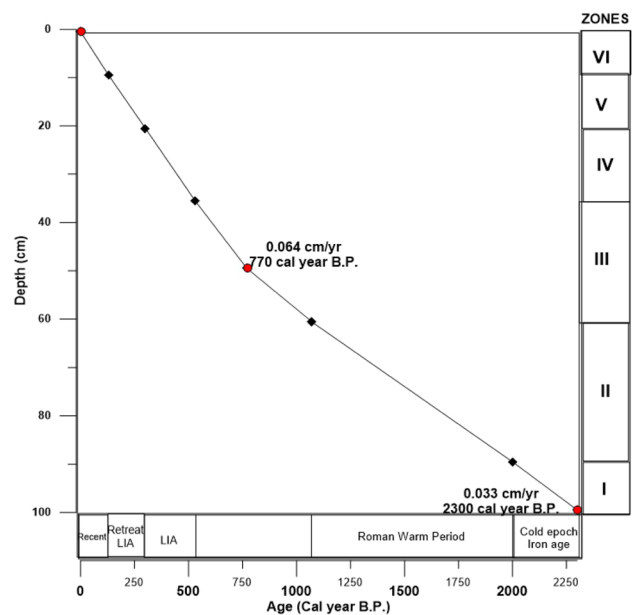
86.364%, 13.636 to 46.667% and 0 to 23.237% respectively, with the average value of 7.352%, 60.091%, 28.893% and 3.665% respectively. Kaolonite and illite constitute more than 85% and illite was the dominant clay mineral throughout the core length (Fig. 4). Smectite and kaolinite showed an increasing trend whereas illite showed a decreasing trend from 2300 to 2000 cal yr BP in zone I. From 2000 to 1070 cal yr BP in zone II, smectite, kaolinite, and chlorite fluctuated along with the average while illite maintained lower than average except at 62 cm (1160 cal yr BP) wherein it showed a positive peak. Kaolinite fluctuated along the average and chlorite was constant with lower than the

Table 4 Range and average values of clay minerals, illite chemistry, smectite crystallinity and illite crystallinity

Depth (cm)		Illite (%)	Kaolinite (%)	Smectite (%)	Chlorite (%)	Illite chemistry	Smectite Crystallinity	Illite crystallinity
	Core Min	43.537	13.636	0.000	0.000	0.571	2.000	0.200
	Core Max	86.364	46.667	20.745	23.237	0.031	0.333	0.200
	Core Avg	60.091	28.893	7.352	3.665	0.373	0.944	0.200
0–9	Zone VI Avg	62.540	27.170	6.090	4.200	0.356	1.257	0.200
10–21	Zone V Avg	56.488	25.112	13.734	4.666	0.358	1.475	0.200
22–35	Zone IV Avg	61.210	30.534	5.293	2.962	0.392	0.556	0.200
36–61	Zone III Avg	65.356	28.312	5.693	0.639	0.372	1.197	0.200
62–91	Zone II Avg	54.979	29.349	9.365	6.307	0.534	0.567	0.200
92–100	Zone I Avg	61.355	32.212	3.458	2.975	0.415	1.142	0.200

average value from 1070 to 530 cal yr BP in zone III. Smectite in the lower portion (52 cm to 61 cm i.e. from 860 to 1130 cal yr BP) was higher than the average (Fig. 4) which then decreased to less than average in the upper portion (36 cm to 52 cm i.e., from 560 to 860 cal yr BP). Illite compensated for smectite in this zone. From 530 to 300 cal yr BP in zone IV chlorite and kaolinite fluctuated along the average while, smectite showed an increasing trend and illite largely compensated smectite. From 300 to 130 cal yr BP in zone V, kaolinite and chlorite showed higher fluctuations along with the average while smectite showed an increasing trend. Illite maintained largely lower than the average. In the upper zone VI from 130 cal yr BP to present, smectite showed a decreasing trend and illite compensated smectite. Kaolinite and chlorite fluctuated along with the average.

Geochemistry

The range and average of elemental concentration for core GC 13 are presented in Table 5. The elements Al, Ti, Fe, Mn, Pb, and Zn varied in the core in the range from 6.846 to 14.738%, 0.246–1.181%, 2.305–6.142%, 171.375–459.325 ppm, 0–5.757 ppm, and 57.650–1276.200 ppm, with the average values of 12.448%, 0.776%, 4.780%, 362.675 ppm, 0.933 ppm, and 302.507 ppm respectively. Abundance of average elemental value in the core GC-13 is in the order Al > Fe > Ti > Mn > Zn > Pb (Table 5). The vertical distribution of elements when considered, all the major elements viz. Fe, Mn, Al, and Ti showed similar trends with a positive peak at 96 cm i.e. at 2190 cal yr BP and a sharp negative peak at 94 cm i.e., at 2130 cal yr BP in the zone I i.e., from 2300 to 2000 cal yr BP. The Pb was constant and Zn showed a lower value than average except a positive peak at 90 cm i.e., at 2010 cal yr BP. Iron and Mn showed similar trends from 2000 to 1070 cal yr BP in zone II with slightly higher values in the middle of the zone, whereas, Al in the lower part of the zone was lower than the average, and in the upper part it was higher than the average (Fig. 4). The trend of Ti and also Zn was fluctuating and higher than the average in this zone, while Pb was constant

Table 5 Range and average values of metals concentration and Mn/Fe

Depth (cm)		Al (%)	Ti (%)	Fe (%)	Mn (ppm)	Pb (ppm)	Zn (ppm)	Mn/Fe
	Core Min	6.846	0.246	2.305	171.375	0.000	57.650	0.006
	Core Max	14.738	1.181	6.142	459.325	5.757	1276.200	0.010
	Core Avg	12.448	0.776	4.780	362.675	0.933	302.507	0.008
0–9	Zone VI Avg	12.420	0.840	5.141	391.435	1.548	257.440	0.0076
10–21	Zone V Avg	12.526	0.938	5.244	387.900	1.130	219.625	0.0074
22–35	Zone IV Avg	13.518	0.750	4.789	395.332	1.312	396.575	0.0083
36–61	Zone III Avg	12.713	0.561	4.447	352.221	1.497	171.248	0.0080
62–91	Zone II Avg	12.339	0.883	4.878	352.183	0.288	476.750	0.0072
92–100	Zone I Avg	10.522	0.793	4.419	316.575	0.025	133.880	0.0072
	PAAS	9.94	0.6	5	900	20	85	
	Continental crustal values	8.23	0.57	5.63	950	12.5	70	

PAAS values were given by Taylor and McLennan (1985) and continental crust values were proposed by Taylor (1964)

and lower than average. From 1070 to 530 cal yr BP in zone III, Fe, Mn, and Zn showed similar lower than the average values, while Al and Pb showed higher values. Titanium was higher than average in the lower portion and showed a sudden decrease at 50 cm i.e., at 770 cal yr BP and further, remained lower than the average. The elements Al, Ti, Fe, Mn, and Pb showed an increasing trend while Zn showed a positive peak in the lower part of the zone IV i.e., from 530 to 300 cal yr BP. From 300 to 130 cal yr BP in Zone V, Fe, Mn, Al, Ti, Pb displayed higher than average values and a decreasing trend, while, Zn maintained lower than average value. From 130 cal yr BP to present in zone VI, Fe, Mn, Ti, and Pb showed higher than average values and decreased at the surface. Aluminium fluctuated around the average value with a decrease at the surface. Zinc exhibited a slight positive peak in the lower part of this zone followed by a decrease at the surface.

Discussion

Depositional environment with time from sediment components

The top 100 cm of the sediment core GC-13 constitutes more than 95% of finer sediments (silt and clay) suggesting that the deposition of sediments took place largely from suspension mode. Further, the core exhibited six distinct zones of depositional environments from bottom to surface based on the distribution of sediment components, clay minerals, and metals and are numbered as zone I, zone II, zone III, zone IV, zone V and zone VI (Fig. 4; Table 2).

The ternary diagram of sediment components (Fig. 3) indicated a close cluster of zone II and zone V, as well as zone III and VI indicating similar hydrodynamic conditions and sediment depositional environments. The lower average value of silt from 2000 to 1070 cal yr BP in zone II (55.792%) and from 300 to 130 cal yr BP zone V (64.380%) (Table 2) compared to the overall average silt (66.105%) of the core and higher average clay (43.598% and 35.281%) in these zones compared to overall average clay (33.386%) suggests the prevalence of low energy conditions when the sediment deposited in these zones during the corresponding chronological period. From 1070 to 530 cal yr BP in zone III and from 130 cal yr BP to present in zone VI, higher average silt i.e., 69.579% and 67.952% (Table 2) respectively compared to average silt of the core and lower average clay values 30.007% and 31.740% respectively than core average clay reveals the presence of higher energy conditions when the sediment deposited in these zones during the corresponding chronological period. This indicates that there was a repetition of the similar depositional environments in zone II and zone V i.e., from 2000 to 1070 cal yr BP

and from 300 to 130 cal yr BP, and also in zone III and VI i.e., from 1070 to 530 cal yr BP and from 130 cal yr BP to present.

The estimated age – chronology (Fig. 5) revealed that zone I (2300–2000 cal yr BP), zone II (2000–1070 cal yr BP and part of zone III (from 1070 up to 770 cal yr BP) experienced relatively lower rates of sedimentation, while the upper part of zone III (from 770 up to 530 cal yr BP), zone IV (530–300 cal yr BP), zone V (300–130 cal yr BP) and zone VI (130 cal yr BP to present) has experienced a higher rate of sedimentation. Relatively higher silt (Table 2) was associated with zone I, zone III, zone IV, and zone VI, the highest being in zone IV i.e. from 530 to 300 cal yr BP, suggesting higher input of silt during the period. High input of silt in zones III, IV, and VI, seems to be responsible for the higher rate of sedimentation in these zones. High silt and low clay content must have facilitated relatively high porosity and therefore, comparatively better oxic conditions.

Source and changing energy conditions with time from clay minerals

In core GC-13, illite was the dominant clay mineral, and illite and kaolinite together contributed more than 80% of clay minerals. The abundance of clay minerals was in the order of illite > kaolinite > smectite > chlorite. The dominance of illite indicated its contribution from the felsic rocks of Archean Proterozoic Gneiss Complex (Mazumdar et al. 2015). Illite is generally of detrital origin (Ehrmann et al. 2011) and is widely formed by physical weathering in colder regions from muscovite mica (Weaver 1989). The Himalayan mountain chain comprises abundant muscovite mica, phyllites, schists, and shales (Heim and Gansser 1939) which on weathering must have formed illite which was later transported by the Ganga and Brahmaputra rivers to the Bay of Bengal. Kolla and Biscaye (1973) and Rao and Rao (1977) stated that the turbidity currents of these rivers have transported illite towards the south possibly up to the study area. The second most abundant clay mineral, kaolinite was majorly formed due to chemical weathering from Archean granites, gneisses, charnockites, and khondalites in a tropical climatic condition. Low smectite content in the core may be due to the limited availability of Deccan Basalt, resulting in weathering products namely black cotton soil in the catchment area. Low chlorite in the humid and tropical region was attributed to its unstable nature (Diju and Thamban 2006).

Further, clay minerals have been used to understand the hydrodynamic conditions (Moore and Reynolds 1989; Liu et al. 2010; Aksu et al. 1998). It is well established that illite and kaolinite due to their coarser size, deposit under high energy conditions, and smectite with comparatively finer size gets deposited under low energy conditions (Oliveria et al. 2002). In core GC-13, more than 80% of clay

minerals constitute illite and kaolinite suggesting deposition of coarser size clay minerals in high energy conditions. Average illite, smectite, and kaolinite + chlorite of each zone plotted on a ternary diagram (Fig. 6), was employed to understand the variation in paleo hydrodynamic energy conditions. The cluster of zones II and V and zones III and VI supported similar hydrodynamic energy conditions that prevailed during sedimentation, as interpreted using sediment components. Along the length of sediment core GC-13, from 2300–2000 cal yr BP in the zone I, all the clay minerals fluctuated while Kaolinite was overall higher than average and illite displayed a drastic decreasing trend, similar to that of sand, suggesting the prevalence of decreasing energy conditions. Average illite value from 2000–1070 cal yr BP in zone II was 4.979% and from 300 to 130 cal yr BP in zone V 56.488% (Table 4) was lower than the overall illite (avg. 60.091%) of the core whereas smectite average 9.365% and 13.734%, respectively in these zones was higher than overall smectite average 7.352%, suggesting low energy conditions. In zone III (from 1070 up to 530 cal yr BP) and zone VI (from 130 cal yr BP to present) the average concentration of illite was 65.356% and 62.540%, respectively, was higher than the average illite of the core, whereas smectite average was 5.693% and 6.090% respectively in these zones was lower than the smectite overall average implying higher energy conditions. This strongly supports the interpretations made based on depositional environments using sediment components except for zone IV.

Illite crystallinity, smectite crystallinity, and illite chemistry calculated for the core to identify the source and degree of weathering presented in Table 4 indicated uniform 0.2 Illite crystallinity which suggests the presence of
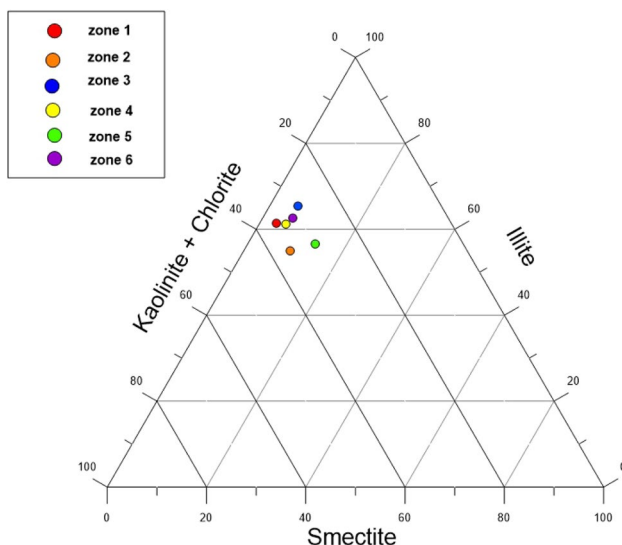
highly crystalline illite. Blenkinsop (1988) and Verdel et al. (2011) have reported that illite crystallinity values below 0.25 suggest a significant contribution from rocks that have undergone incipient to epigenetic grade metamorphism. The highly crystalline illite recorded in the core might be due to the transformation of smectite to illite (Mazumdar et al. 2015; Bejugam and Nayak 2017). All the zones except zone II and zone IV have smectite crystallinity between 1 and 1.5 (Table 4) suggesting the presence of crystalline smectite (Ehrmann et al. 2005), while in zone II (from 2000 to 1070 cal yr BP) and IV (from 530 to 300 cal yr BP) smectite crystallinity is below 1 suggesting highly crystalline smectite, thus indicating poor hydrolyzation of smectite due to poor rainfall and temperature conditions (Bejugam and Nayak 2017; Thamban et al. 2002) in zone IV. Further, except for zone II (from 2000–1070 cal yr BP), all the zones have illite chemistry below 0.5 suggesting the source to be Fe–Mg rich rocks that are supplied through strong physical weathering from the Himalayan region. While in zone II, illite chemistry was above 0.5 indicating Al-rich illite through hydrolysis during weathering probably leached from felsic rocks of the Eastern Ghats (Bejugam and Nayak 2017). Further, in zone II supply from Al-rich illite and higher than average smectite along with highly crystalline smectite suggest decreased input from the Himalayan region.

Source and changing depositional conditions with time from elements

The average concentrations of Al in different rock types differ by about 10% from the average crustal value (Taylor and McLennan 1985; Turekian and Wedepohl 1961). Therefore, they are used as indicators of lithogenous sources and to quantify the deposition of the lithogenic components (Murray and Leinen 1996). Al was the dominant element in core GC-13 and the average concentration of Al was higher than that of continental crust and Post Archean Australian shale (PAAS) implying a supply of abundant aluminosilicate minerals from the felsic rocks. Mazumdar et al. (2015) had earlier suggested that the sediment source off Mahanadi was dominated by felsic rocks. The average Fe value in the core was close to the PAAS value with a difference of only 0.23%, while the average Fe was lower than the continental crust value. Ti value was slightly higher than PAAS and continental crust value. Mn was the least available major element in the core. The average Mn value was lower than PAAS and continental crust. Fe and Ti are generally associated with mafic rocks. Thus, a lower concentration of Fe and Mn, with slightly higher Ti than standards in the core GC-13 suggested less supply from mafic rocks. Among the major elements, Al and Ti exhibited a similar trend in the vertical distribution supporting terrigenous input. Ti from 50 to 35 cm showed similar distribution to that of smectite with

Fig. 6 Ternary diagram for classification of hydrodynamic conditions using clay minerals

high values in the lower part of zone III suggesting relatively higher input from mafic source rock during the period. Fe and Mn showed similar profiles throughout the core which implies their similar redox behaviour.

Further, to understand the association of metals with the sediment component and clay minerals Pearson's correlation (Table 6) analysis was carried out. Al showed a strong correlation with Fe, Mn, and Pb indicating that these metals were associated with aluminosilicate minerals supporting their terrigenous source and suggesting similar post-depositional behaviour. Ti showed a good correlation with Fe, Fe with Mn, and Mn with Pb. Further, Mn showed a significant correlation with silt supporting their lithogenic source. Smectite, Kaolinite, and Chlorite showed a strong negative correlation with illite indicating different source rock, hydrodynamic conditions, and climate. Smectite showed a positive correlation whereas illite showed a strong negative correlation with Ti indicating the source of Ti and smectite as basic igneous rocks.

Geochemical elements in sediments are not only an important proxy to identify the source, but also for understanding depositional processes and climate. In the studied core with depth all the major elements viz. Fe, Mn, Al, and Ti exhibited similar trends with a positive peak at 2190 cal yr BP (96 cm) and a sharp negative peak at 2130 cal yr BP (94 cm) in zone I i.e. from 2300 to 2000 cal yr BP, indicating supply of sediment from lithogenous rocks primarily from continental sources. From 2000 to 1070 cal yr BP in zone II Fe and Mn showed a similar trend with slightly higher values in the middle of the zone and Ti and Zn showed a fluctuating trend with higher than the average in this zone. Similarly from 300 to 130 cal yr BP in Zone V, Fe, Mn, Ti showed higher than average values and a decreasing trend, while, Zn maintained lower than average values. The presence of high

clay content, smectite percentage, Ti, Fe along with Mn and Zn supports increased terrestrial material supply from 2000 to 1070 cal yr BP and 300 to 130 cal yr BP periods to the Bay of Bengal. Both southwest (SW) and northeast (NE) monsoons with varying intensities and characteristics drain the Indian sub-continent and release sediments to the Bay of Bengal. High Ti concentrations and significant association of Fe and Ti in sediments derived from Krishna River were earlier related to the Deccan trap basalts source as they are rich in titanium (Das and Krishnaswami 2007; Bejugam and Nayak 2017; Kangane et al. 2019). A significant correlation obtained between Ti and smectite and also between Ti and Fe supports their strong association in the sediments. Increased smectite content along with high Ti and Fe suggests increased chemical weathering of mafic rocks possibly due to the intensification of southwest monsoon in the presence of a warm and wet climate (Sridhar 2009; Suokhrie et al. 2018). Increased rainfall in the Indian subcontinent during warm periods was documented earlier by Pothuri et al. (2014) and Pothuri (2017). The sediment material brought by the rivers during this period was distributed and the hydrodynamic conditions at the core site facilitated the deposition of higher clay, fine clay mineral smectite preserving high Ti and Fe.

In zone III from 1070 to 530 cal yr BP Al and Pb values were higher than the average and in zone VI, from 130 cal yr BP to present, Pb values were higher than average and decreased at the surface, Al, however, fluctuated around the average value with a decrease at the surface. Fe, Mn, and Zn values were lower than average and Ti higher than average in the lower portion but showed a sudden decrease at 50 cm i.e., at 770 cal yr BP and further, remained lower than the average in zone III. Low Fe, Mn, Zn, Ti in this zone indicated the reduced release of

Table 6 Pearson's correlation between sediment component, clay minerals and metals

	Sand	Silt	Clay	Illite	Kaolinite	Smectite	Chlorite	Al	Ti	Fe	Mn	Pb	Zn
Sand	1.000												
Silt	−0.086	1.000											
Clay	0.054	**−0.999**	1.000										
Illite	0.056	0.015	−0.016	1.000									
Kaolinite	−0.076	0.227	−0.225	**−0.629**	1.000								
Smectite	−0.081	−0.152	0.155	**−0.665**	0.062	1.000							
Chlorite	0.101	−0.160	0.157	**−0.311**	−0.214	−0.021	1.000						
Al	**−0.351**	0.266	−0.255	0.094	−0.119	0.001	−0.026	1.000					
Ti	−0.024	−0.030	0.030	**−0.593**	0.218	**0.530**	0.229	0.139	1.000				
Fe	−0.153	0.134	−0.129	−0.172	−0.050	0.231	0.127	**0.488**	**0.461**	1.000			
Mn	**−0.347**	**0.325**	**−0.314**	0.089	−0.157	−0.006	0.049	**0.645**	0.183	**0.754**	1.000		
Pb	**−0.318**	0.204	−0.195	**0.416**	−0.175	**−0.314**	−0.206	**0.373**	**−0.504**	−0.015	**0.294**	1.000	
Zn	−0.018	0.009	−0.008	−0.103	−0.020	0.110	0.100	0.022	0.211	0.233	0.261	−0.160	1.000

Marked correlations are significant at $p < 0.05000$ N = 47

material from the Peninsula Rivers and reduced intensity of the southwest monsoon. In zone VI Fe, Mn, Ti values were higher than the average value and decreased at the surface, while Zn exhibited a slight positive peak in the lower part of this zone followed by a decrease at the surface. High Fe, Mn, and Ti in zone VI may be due to their release in recent years by human-induced processes. High Pb in sediments supports the influence of anthropogenic activity. High Al, Pb with high silt and illite indicated an association of Al and Pb with illite. A good correlation obtained between illite and Pb supports their association. Sediment with high Al, therefore, must have been supplied either from the Himalayan Mountain rocks rich in muscovite mica or acidic rocks of the Mahanadi catchment area or both. The geology of Mahanadi River along its course consists of acidic igneous rocks viz. khondalites, charnockites, granites, gneisses along with limestones, sandstones, and shales of Gondwanas (Chakrapani and Subramanian 1990). Illite generally forms through physical weathering in cold regions in arid climatic conditions from muscovite (Weaver 1989). Therefore, illite must have been released either from muscovite mica from cold climate or through high-grade metamorphism of acidic igneous rocks (Kolla and Rao 1990). The high content of illite along with Al present in zones III and VI strongly supports their formation mainly in a cold climate and released from the rocks in the Himalayan Mountains during the intensified northeast monsoon. Relatively high hydrodynamic conditions during the above periods in the studied core site facilitated the deposition of higher silt, coarse clay mineral illite preserving high Al and Pb. In zone IV i.e., from 530 to 300 cal yr BP the elements Al, Ti, Fe, Mn and Pb showed an increasing trend while Zn showed a positive peak in the lower part indicating a higher supply of sediment-rich in metals.

High Mn was associated with zones with higher silt namely zone IV (530–300 cal yr BP), zone VI (130 cal yr BP to present), and, to some extent, zone III (1070–530 cal yr BP). Similarly, Zn was also high in these zones in addition to zone II (2000–1070 cal yr BP). It is well known that Mn forms oxyhydroxide in oxic conditions and Zn is generally associated with Mn (Bejugam and Nayak 2017). The sediments brought from land along with high silt must have reduced the intensity of the Oxygen Minimum Zone facilitating the deposition of higher Mn and Zn in the studied sediment core. Further, the coarser sediments with high porosity allow for the remobilization of metals. In deeper, low oxygenated conditions, Mn is reduced faster than Fe giving rise to lower Mn/Fe ratios while in coarser oxygenated conditions higher Mn accumulation takes place leading to higher Mn/Fe ratios. Therefore, the Mn/Fe ratio is a reliable proxy used to understand the OMZ (Naeher et al. 2013). In core GC-13, lower Mn/Fe ratios and silt indicated the presence of lower oxygen concentrations in zone II and zone V, while, higher Mn/Fe ratios and silt content support high oxygen availability in zone III and VI (Table 5).

Climatic evolution during the last 2300 cal yr BP

Holocene climate experienced drastic variations and is represented by the Holocene Climate Optimum (HCO), Medieval Warm Period, Little Ice Age, Modern Warm Period, and many other minor perturbations at different locations on the earth. Earlier, cyclicity in climate variation during the Holocene had been reported by Bond and Lotti (1995), Broecker and Hemming (2001), Burroughs (2003). Bond and Lotti (1995) have stated that the iceberg calving cycles correlate with warm-cold oscillations. Heinrich (1988) observed in the eastern North Atlantic, six discreet layers of sediment-rich ice-rafted debris in a deep-sea sediment core. These studies proved that there were climatic variations between cold and warm oscillations. The environmental and hydrodynamic conditions of climatic changes between cold and warm oscillations are expected to bring corresponding changes in conditions of sediment deposition.

When the zones in the sediment core studied are related to Holocene climate divisions, Zone I from 2300–2000 cal yr BP represents the Cold Epoch and Iron Age of 900–300 BC and zone II from 2000 to 1070 cal yr BP represents Roman Warm Climate which occurred between 250 BC and 400 AD and early Medieval Warm Period. However, the effects of the Medieval Warm Period from 900–1300 AD were supported by high smectite only in the lower part of zone III. Zone IV from 530 to 300 cal yr BP represents the Little Ice Age of 1350–1550 AD and the retreating phase of the Little Ice Age from 1550 to 1850 AD was represented by zone V from 300 to 130 cal yr BP. The zone VI from 130 cal yr BP to present seems to be influenced by human-induced climate change and represents a higher release of silt, illite, Al, and Pb due to the melting of Himalayan glaciers because of the increase in temperature in the recent years.

During the Iron Age – cold epoch (2300–2000 cal yr BP), cold and dry conditions have been regionally recognized through shifts from wetter conditions to gradual drier conditions (Ponton et al. 2012) and weaker summer monsoons (Naidu et al. 2020) and globally by Drake (2012) who reported that arid conditions prevailed in the Mediterranean Sea based on changes in warm species dinocysts and foraminifera. In the Roman Warm Period (2000–1070 cal yr BP), increased clay indicated lower hydrodynamic conditions and the presence of higher smectite and Ti suggested warm—wet conditions and increased southwest monsoons responsible for increased input of finer sediments from mafic igneous rocks. Regionally, increased southwest monsoons have been documented during the Roman Warm Period with a reduction in illite concentration in sediments. During this

period earlier studies have recorded a decrease in illite and suggested reduced fluvial influx (Chauhan et al. 2004), an increase of Ti indicated an increase in SW monsoon (Thamban et al. 2007) and high negative ɗ $^{18}O_w$ values suggested high summer monsoon (Naidu et al. 2020). Globally, Martin—Puertas et al. (2009) reported the high humid period with warmer temperature and moderate precipitation in Zonar Lake.

From ninth to the fourteenth century A.D., a climate warmer than that which prevailed around the twentieth century was observed by Hughes and Diaz (1994), and this epoch was named the Medieval Warm Period, as it coincides with the Middle Ages in Europe. The most recent and significant climate transition from the medieval warm period up to the little ice age was observed in the late Holocene (Hughes and Diaz 1994; Crowley and Lowery 2000; Bradley et al. 2003; Holzhauser et al. 2005). In the present study, the period from 1070 to 530 cal yr BP showed an increase in silt and illite content reflecting increased hydrodynamic conditions and the presence of high illite suggested cold and dry climate conditions. However, earlier studies (Kuppusamy and Ghosh 2012; Surokhrie et al. 2018; Naidu et al. 2020) have reported intensified southwest monsoons and warm–wet periods for the Bay of Bengal. Mann et al. (2009) reported warmer conditions equal to or more than the past decade but well below recent levels at the global level.

Zone IV from 530 to 300 cal yr BP of the studied core with high silt and illite showed clear evidence of the colder and dry conditions that characterized the Little Ice Age (LIA). An increase in the silt and illite input suggested an increase in hydrodynamic conditions and weaker southwest monsoons. During this period, Singhvi and Kale (2010) have reported the presence of cool and dry conditions and weakening of the SW monsoon and Kuppusamy and Ghosh (2012) have reported the period as the weakest southwest monsoon. Surokhrie et al. (2018) reported a sudden increase in angular asymmetric benthic foraminifera which indicated a decrease in monsoon, less freshwater influx, and less coarse material, and Naidu et al. (2020) have reported a high positive ɗ$^{18}O_w$ value which suggested weaker summer monsoon during this period. Anderson et al. (2016) reported that the cooling over Eurasia during LIA was responsible for weakened the SWM and Easterbrook (2016) has reported decreased river flux during the ice age. However, in zone IV i.e. from 530 to 300 cal yr BP, the highest input of silt was noted. Studies on both continents and adjacent oceans have shown that there were increased dust fluxes during the glacial periods. The increased dust flux was recorded in most loess deposits on land with silt-sized particles (Pye 1987; Muhs and Bettis 2003). Stoll et al. (2007) reported that part of the shift to higher mean εNd throughout the Bay during glacial maxima may also arise from a uniform increase in deposition of far-field dust from Arabian and Persian Gulf

regions. The higher aeolian flux during glacial times in the continental margin sediments off Pakistan was recorded by von Rad et al. (1999). They had also reported that the aeolian input generally decreased from glacial to interglacial times and strong riverine input and mobilization of fine-grained sediment coinciding with rapid deglacial sea-level rise.

During retreating LIA (300–130 cal yr BP), a slight increase in temperatures lead to an increase in clay, smectite, and Ti indicated reduced hydrodynamic conditions. An increase in smectite and Ti suggested warm–wet conditions and intensified southwest monsoon strongly supports additional input of finer sediments from mafic igneous rocks. Since the onset of recent times (130 cal yr BP to present), a significant decline in southwest monsoon occurred due to global warming (Satyanarayana et al. 2019). However, increased silt and illite along with Ti, Fe Mn, and Pb suggest an increase in hydrodynamic conditions and high sediment discharge. This was related to the recent rise in global temperature leading to the melting of Himalayan glaciers. Bradley and Jonest (1993) observed that a gradual increase in warmer conditions may be due to the relative absence of major volcanic eruptions and a high level of greenhouse gases.

Conclusions

The sediment gravity core retrieved at Latitude 18º 99′N and Longitude 85º 38′E from the western Bay of Bengal at 260.2 m water depth off Mahanadi indicated changing depositional environments from ~2300 years BP to present. Six zones of distinct depositional environments of varying hydrodynamic conditions were identified based on the distribution of sediment components and clay minerals. Similar hydrodynamic condition of zone II (2000 years BP to 1070 cal yr BP) and zone V (300–130 cal yr BP) and also between zone III (1070–530 cal yr BP) and VI (132 cal yr BP to present) revealed reoccurrence of the similar depositional environments with time. Changes in release and intensity of source materials are reflected in response to changes in the south monsoon intensity viz. cold and dry conditions with the weaker southwest monsoon in Zone III and VI and warm and wet conditions are reflected in zone II and V with the intense southwest monsoon. Changes in the intensity of OMZ based on variation in hydrodynamic conditions and the depositional environments were recorded. The variations in the paleo-depositional environment controlled by the hydrodynamic conditions in the studied area were regulated by the changes in climatic controlled monsoons and the release of material from the source areas with time. A climate change model from 2300 cal yr BP to present was discussed along with the regional and global scenarios.

References

Aksu AE, Yasar D, Orhan USLU (1998) Assessment of marine pollution in Izmir Bay: Heavy metal and organic compound concentrations in surficial sediments. Turk J Eng Environ Sci 22(5):387–416

Alagarsamy R, Zhang J (2005) Comparative studies on trace metal geochemistry in Indian and Chinese rivers. Curr Sci 89(2):299–309

Anderson DM, Overpeck JT, Gupta AK (2002) Increase in the Asian southwest monsoon during the past four centuries. Science 297(5581):596–599

Avinash K, Kurian PJ, Warrier AK, Shankar R, Vineesh TC, Ravindra R (2016) Sedimentary sources and processes in the eastern Arabian Sea: insights from environmental magnetism, geochemistry and clay mineralogy. Geosci Front 7(2):253–264

Banerjee B, Ahmad SM, Babu EVSSK, Padmakumari VM, Beja SK, Satyanarayanan M, Krishna AK (2019) Geochemistry and isotopic study of southern Bay of Bengal sediments: implications for provenance and paleoenvironment during the middle Miocene. Palaeogeogr Palaeoclimatol Palaeoecol 514:156–167

Bejugam P, Nayak GN (2017) Source and depositional processes of surface sediments and their implications on productivity in recent past off Mahanadi to pennar river mouths, western Bay of Bengal. Palaeogeogr Palaeoclimatol Palaeoecol 483:58–69

Benshila R, Durand F, Masson S, Bourdallé-Badie R, de Boyer Montégut C, Papa F, Madec G (2014) The upper Bay of Bengal salinity structure in a high-resolution model. Ocean Model 74:36–52

Biscaye PE (1965) Mineralogy and sedimentation of recent deep-sea clay in the Atlantic Ocean and adjacent seas and oceans. Geol Soc Am Bull 76(7):803–832

Blenkinsop TG (1988) Definition of low-grade metamorphic zones using illite crystalinity. J Metamorph Geol 6(5):623–636

Bond GC, Lotti R (1995) Iceberg discharges into the North Atlantic on millennial time scales during the last glaciation. Science 267(5200):1005–1010

Bradley RS, Jonest PD (1993) 'Little Ice Age' summer temperature variations: their nature and relevance to recent global warming trends. The Holocene 3(4):67–376

Bradley RS, Hughes MK, Diaz HF (2003) Climate in medieval time. Science 302(5644):404–405

Broecker WS, Hemming S (2001) Climate swings come into focus. Science 294(5550):2308–2309

Burroughs WJ (2003) Weather cycles: real or imaginary? Cambridge University Press, Cambridge, UK

Calvert SE, Pedersen TF (1993) Geochemistry of recent oxic and anoxic marine sediments: implications for the geological record. Mar Geol 113(1–2):67–88

Chakrapani GJ, Subramanian V (1990) Preliminary studies on the geochemistry of the Mahanadi River basin, India. Chem Geol 81:241–253

Chauhan, O.S., Patil, S.K. and Suneethi, J., 2004. Fluvial influx and weathering history of the Himalayas since Last Glacial Maxima–isotopic, sedimentological and magnetic records from the Bay of Bengal. *Current Science,* 509–515.

Crowley, T.J. and Lowery, T.S., 2000. How warm was the medieval warm period?. *AMBIO: A Journal of the Human Environment,* 29(1), 51–54.

Das A, Krishnaswami S (2007) Elemental geochemistry of river sediments from the Deccan Traps, India: implications to sources of elements and their mobility during basalt–water interaction. Chem Geol 242(1):232–254

Datta DK, Gupta LP, Subramanian V (2000) Dissolved fluoride in the lower Ganges-Brahmaputra-Meghna river system in the Bengal Basin Bangladesh. Environ Geol 39(10):1163–1168

Demina LL, Novichkova EA, Lisitzin AP, Kozina NV (2019) Geochemical signatures of paleoclimate changes in the sediment cores from the Gloria and Snorri Drifts (Northwest Atlantic) over the Holocene-Mid Pleistocene. Geosciences 9:432–450

Dessai DVG, Nayak GN (2007) Seasonal distribution of surface sediments and hydrodynamic conditions of Zuari estuary, Goa, Central west coast of India. J Ind Assoc Sedimentol 26(1–2):25–32

Diju S, Thamban M (2006) Clay mineral and textural variations in the sediments of Chandragiri River, estuary and shallow marine realms off Kasaragod, Kerala. J Geol Soc India 67:189–196

Dixit PR, Kar B, Chattopadhyay P, Panda CR (2013) Seasonal variation of the physicochemical properties of water samples in Mahanadi Estuary. East Coast of India, India

Drake BL (2012) The influence of climatic change on the Late Bronze age collapse and the Greek dark Ages. J Archaeol Sci 39(6):1862–1870

Easterbrook DJ (2016) Evidence-based climate science (Second Edition): cause of global climate changes: correlation of global temperature, sunspots, solar irradiance, cosmic rays, and radiocarbon and beryllium production rates. Elsevier, Netherlands, pp 245–262

Ehrmann W, Setti M, Marinoni L (2005) Clay minerals in Cenozoic sediments of Cape Roberts (McMurdo Sound, Antarctica) reveal palaeoclimatic history. Palaeogeogr Palaeoclimatol Palaeoecol 229(3):187–211

Ehrmann W, Hillenbrand CD, Smith JA, Graham AG, Kuhn G, Larter RD (2011) Provenance changes between recent and glacial-time sediments in the Amundsen Sea embayment, West Antarctica: clay mineral assemblage evidence. Antarct Sci 23(5):471–486

Fleitmann D, Burns SJ, Mudelsee M, Neff U, Kramers J, Mangini A, Matter A (2003) Holocene forcing of the Indian monsoon recorded in a stalagmite from southern Oman. Science 300:1737–1739

Folk RL (1968) Petrology of sedimentary rocks. Hemphill Publishing Company, Texas

Frey M (1987) Very low grade metamorphism of clastic sedimentary rocks. Low Temperature Metamorphism Blackie, London, pp 9–58

Gasse F, Fontes JCh, Van Campo E, Wei K (1996) Holocene environmental changes in Bangong Co basin (western Tibet). Part4: discussions and conclusions. Palaeogeogr Palaeoclimatol Palaeoecol 120:79–82

Hart GF (1999) The deltas of peninsular India. Retrieved from http://www.geol.Isu.edu/WDD/PUBLICATIONS/HartIndrpt00/india.html.

Heim A, Gansser A (1939) Central himalaya geological observations of swiss expedition. Hindustan Publishing corporation, India, pp 1–246

Heinrich H (1988) Origin and consequences of cyclic ice rafting in the Northeast Atlantic Ocean during the past130,000 years. Quatern Res 29(2):142–152

Holzhauser H, Magny M, Zumbuühl HJ (2005) Glacier and lake-level variations in west-central Europe over the last 3500 years. Holocene 15(6):789–801

Hughes MK, Diaz HF (1994) Was there a 'medival warm period', and if so where and when? Climatic Change 26(2–3):109–142

Jarvis I, Jarvis KE (1985) Rare-earth element geochemistry of standard sediments: a study using inductively coupled plasma spectrometry. Chem Geol 53:335–344

Kangane J, Nayak GN, Choudhary S (2019) Source and processes from core sediment samples off Mahanadi and Krishna rivers, western Bay of Bengal. J Indian Assoc Sedimentol 36(1):65–83

Kolla V, Biscaye PE (1973) Clay mineralogy and sedimentation in the eastern Indian Ocean. Deep Sea Res 20(8):727–738

Kolla V, Rao NM (1990) Sedimentary sources in the surface and near-surface sediments of the Bay of Bengal. GeoMarine Lett 10(3):129–135

Konhauser KO, Powell MA, Fyfe WS, Longstaffe FJ, Tripathy S (1997) Trace element geochemistry of river sediment, Orissa State India. J Hydrol 193(1–4):258–269

Kuppusamy M, Ghosh P (2012) Cenozoic climatic record for monsoonal rainfall over the Indian region. Modern Climatol 1:257–268

Levitus S, Boyer TP (1994) World Ocean Atlas temperature (No. PB-95-270112/ XAB; NESDIS–4) national environmental satellite. Data and Information Service, Washington

Liu Z, Colin C, Li X, Zhao Y, Tuo S, Chen Z, Siringan FP, Liu JT, Huang CY, You CF, Huang KF (2010) Clay mineral distribution in surface sediments of the northeastern South China Sea and surrounding fluvial drainage basins: source and transport. Mar Geol 277:48–60

Mann ME, Zhang Z, Rutherford S, Bradley RS, Hughes MK, Shindell D, Ammann C, Faluvegi G, Ni F (2009) Global signatures and dynamical origins of the little ice age and medieval climate anomaly. Science 326(5957):1256–1260

Martín-Puertas C, Valero-Garcés BL, Brauer A, Mata MP, Delgado-Huertas A, Dulski P (2009) The Iberian-Roman Humid Period (2600–1600 cal yr BP) in the Zoñar Lake varve record (Andalucía, southern Spain). Quatern Res 71(2):108–120

Mazumdar A, Kocherla M, Carvalho MA, Peketi A, Joshi RK, Mahalaxmi P, Joao HM, Jisha R (2015) Geochemical characterization of the Krishna-Godavari and Mahanadi offshore basin (Bay of Bengal) sediments: a comparative study of provenance. Mar Pet Geol 60:18–33

Moore DM, Reynolds RC (1989) X-ray Diffraction and the Identification and Analysis of Clay Minerals. Oxford University Press, Oxford

Muhs DR, Bettis EA III (2000) Geochemical variations in Peoria Loess of western Iowa indicate paleowinds of mid-continental North America during last glaciation. Quat Res 53:49–61

Murray RW, Leinen M (1996) Scavenged excess aluminum and its relationship to bulk titanium in biogenic sediment from the central equatorial Pacific Ocean. Geochim Cosmochim Acta 60(20):3869–3878

Naeher S, Gilli A, North RP, Hamann Y, Schubert CJ (2013) Tracing bottom water oxygenation with sedimentary Mn/Fe ratios in Lake Zurich, Switzerland. Chem Geol 352:125–133

Naidu AS, Han MW, Mowatt TC, Wajda W (1995) Clay minerals as indicators of sources of terrigenous sediments, their transportation and deposition: Bering Basin Russian-Alaskan Arctic. Marine Geol 127(1–4):87–104

Naidu PD, Ganeshram R, Bollasina MA, Panmei C, Nürnberg D, Donges JF (2020) Coherent response of the Indian monsoon rainfall to atlantic multi-decadal variability over the last 2000 years. Scient Rep 10(1):1–11

Nasnodkar MR, Nayak GN (2019) Clay mineralogy and chemistry of mudflat core sediments from Sharavati and Gurpur estuaries: source and processes. Ind J Geo-Marine Sci 48(3):379–388

Oliveira A, Rocha F, Rodrigues A, Jouanneau J, Dias A, Weber O, Gomes C (2002) Clay minerals from the sedimentary cover from the Northwest Iberian shelf. Prog Oceanogr 52(2–4):233–247

Panda UC, Sundaray SK, Rath P, Nayak BB, Bhatta D (2006) Application of factor and cluster analysis for characterization of river and estuarine water systems–a case study: Mahanadi River (India). J Hydrol 331(3–4):434–445

Pejrup M (1988) The triangular diagram used for classification of estuarine sediments: a new approach Tide-influenced sedimentary environments and facies. Reidel publishing company, Dordrecht

Ponton C, Giosan L, Eglinton TI, Fuller DQ, Johnson JE, Kumar P, Collett TS (2012) Holocene aridification of India. Geophys Res Lett 39(3):234

Pothuri D (2017) Indian monsoon rainfall variability during the Common Era: Implications on the ancient civilization. American Geophysical Union, Fall meeting abstract

Pothuri D, Nürnberg D, Mohtadi M (2014) Multi-decadal variation of the Indian monsoon rainfall: implications of ENSO. AGUFM 1:pp43A

Prajith A, Tyagi A, Kurian PJ (2018) Changing sediment sources in the Bay of Bengal: Evidence of summer monsoon intensification and ice-melt over Himalaya during the late quaternary. Palaeogeogr Palaeoclimatol Palaeoecol 511:309–318

PrakashBabu C, Pattan J, Dutta K, Basavaiah N, Ravi Prasad G, Ray DK, Govil P (2010) Shift in detrital sedimentation in the eastern Bay of Bengal during the late quaternary. J Earth Syst Sci 119:285–295

Pye K (1987) Aeolian Dust and Dust Deposits. Elsevier, New York

Rao NVND, Rao MP (1977) Clay mineral distribution in sediments of the eastern part of the Bay of Bengal. Ind J Marine Sci 6(2):166–168

Rao VP, Rao BR (1995) Provenance and distribution of clay minerals in the sediments of the western continental shelf and slope of India. Cont Shelf Res 15(14):1757–1771

Reimer PJ, Bard E, Bayliss A, Beck JW, Blackwell PG, Ramsey CB, Buck CE, Cheng H, Edwards RL, Friedrich M, Grootes PM (2013) IntCal13 and Marine13 radiocarbon age calibration curves 0–50,000 years cal BP. Radiocarbon 55(4):1869–1887

Sarin MM, Borole DV, Krishnaswami S (1979) January. Geochemistry and geochronology of sediments from the Bay of Bengal and the equatorial Indian Ocean. Ind Acad Sci 88:131–154

Satyanarayana GC, Dodla VBR, Srinivas D (2020) Decreasing southwest monsoon rainfall over Myanmar in the prevailing global warming era. Meteorol App 27(1):1816

Singhvi AK, Kale VS (2010) Paleoclimate studies in Indialast ice age to the present. Indian National Science Acad, India

Sridhar A (2009) Evidence of a late-medieval mega flood event in the upper reaches of the Mahi River basin, Gujarat. Curr Sci 23:1517–1520

Stoll HM, Vance D, Arevalos A (2007) Records of the Nd isotope composition of seawater from the Bay of Bengal: implications for the impact of Northern Hemisphere cooling on ITCZ movement. Earth Planet Sci Lett 255:213–228

Stuiver M, Reimer PJ, Reimer RW (2017) CALIB 7.1 [WWW program] at http://calib.org

Sundaray SK, Panda UC, Nayak BB, Bhatta D (2006) Multivariate statistical techniques for the evaluation of spatial and temporal variations in water quality of the Mahanadi river–estuarine system (India)–a case study. Environ Geochem Health 28(4):317–330

Sundaray SK, Nayak BB, Lin S, Bhatta D (2011) Geochemical speciation and risk assessment of heavy metals in the river estuarine sediments—a case study: Mahanadi basin India. J Hazard Mater 186(2–3):1837–1846

Suokhrie T, Saalim SM, Saraswat R, Nigam R (2018) Indian monsoon variability in the last 2000 years as inferred from benthic foraminifera. Quatern Int 479:128–140

Symphonia KT, Nathan DS (2018) Geochemistry and distribution of sediments in the East Indian shelf, SW Bay of Bengal: implications on weathering, transport and depositional environment. J Earth Syst Sci 127(7):96

Taylor SR (1964) Abundance of chemical elements in the continental crust: a new table. Geochim Cosmochim Acta 28(8):1273–1285

Taylor SR, McLennan SM (1985) The continental crust: its composition and evolution. Blackwell Scientific Publications, Oxford

Thamban M, Rao VP, Schneider RR (2002) Reconstruction of late quaternary monsoon oscillations based on clay mineral proxies using sediment cores from the western margin of India. Mar Geol 186(3–4):527–539

Thamban M, Kawahata H, Rao VP (2007) Indian summer monsoon variability during the Holocene as recorded in sediments of the Arabian Sea: timing and implications. J Oceanogr 63(6):1009–1020

Thompson LG, Yao T, Davis ME, Henderson KA, Mosley-Thompson E, Lin P-N, Beer J, Synal H-A, Cole-Dai J, Bolzan JF (1997) Tropical climate instability: the last Glacial cycle from a Qinghai-Tibetanice core. Science 276:1821–1825

Tripathy GR, Singh SK, Ramaswamy V (2014) Major and trace element geochemistry of Bay of Bengal sediments: implications to provenances and their controlling factors. Palaeogeogr Palaeoclimatol Palaeoecol 397:20–30

Turekian KK, Wedepohl KH (1961) Distribution of the elements in some major units of the earth's crust. Geol Soc Am Bull 72(2):175–192

Verdel C, Niemi N, Van Der Pluijm BA (2011) Variations in the illite to muscovite transition related to metamorphic conditions and detrital muscovite content: insight from the Paleozoic passive margin of the southwestern United States. J Geol 119(4):419–437

von Rad U, Schulz H, Riech V, den Dulk M, Berner U, Sirocko F (1999) Multiple monsoon-controlled breakdown of oxygen minimum conditions during the past 30,000 years documented in laminated sediments off Pakistan. Palaeogeogr Palaeoclimatol Palaeoecol 152(1):129–161

Weaver CE (1989) Developments in sedimentology 44: Clays, muds, and shales. Elsevier Science Publisher, Netherlands

Weber ME, Lantzsch H, Dekens P, Das SK, Reilly BT, Martos YM, Meyer-Jacob C, Agrahari S, Ekblad A, Titschack J, Holmes B (2018) 200,000 years of monsoonal history recorded on the lower Bengal Fan-strong response to insolation forcing. Global Planet Change 166:107–119

Yang H, Shi C (2009) Sediment grain size characteristics and its sources of ten wind water coupled erosion tributaries (the ten Kongduis) in the upper Yellow River. Water 11:115–129